# Performance Evaluation of Multi-Vendor Grid-Forming Inverters for Grid-Connected Operation Through Hardware Experimentation

## Preprint

Jing Wang, Subhankar Ganguly, and Benjamin Kroposki

*National Renewable Energy Laboratory*

*Presented at the 2024 IEEE PES T&D Conference & Exposition*
*Anaheim, California*
*May 6–9, 2024*

**NREL is a national laboratory of the U.S. Department of Energy**
**Office of Energy Efficiency & Renewable Energy**
**Operated by the Alliance for Sustainable Energy, LLC**

This report is available at no cost from the National Renewable Energy Laboratory (NREL) at www.nrel.gov/publications.

Contract No. DE-AC36-08GO28308

**Conference Paper**
NREL/CP-5D00-87199
June 2024

# Performance Evaluation of Multi-Vendor Grid-Forming Inverters for Grid-Connected Operation Through Hardware Experimentation

## Preprint

Jing Wang, Subhankar Ganguly, and Benjamin Kroposki

*National Renewable Energy Laboratory*

**Suggested Citation**
Wang, Jing, Subhankar Ganguly, and Benjamin Kroposki. 2024. *Performance Evaluation of Multi-Vendor Grid-Forming Inverters for Grid-Connected Operation Through Hardware Experimentation: Preprint*. Golden, CO: National Renewable Energy Laboratory. NREL/CP-5D00-87199. https://www.nrel.gov/docs/fy24osti/87199.pdf.



**NREL is a national laboratory of the U.S. Department of Energy**
**Office of Energy Efficiency & Renewable Energy**
**Operated by the Alliance for Sustainable Energy, LLC**

This report is available at no cost from the National Renewable Energy Laboratory (NREL) at www.nrel.gov/publications.

Contract No. DE-AC36-08GO28308

**Conference Paper**
NREL/CP-5D00-87199
June 2024

National Renewable Energy Laboratory
15013 Denver West Parkway
Golden, CO 80401
303-275-3000 • www.nrel.gov

## NOTICE

This work was authored by the National Renewable Energy Laboratory, operated by Alliance for Sustainable Energy, LLC, for the U.S. Department of Energy (DOE) under Contract No. DE-AC36-08GO28308. This material is based upon work supported by the U.S Department of Energy Office of Energy Efficiency and Renewable Energy Solar Energy Technologies Office Agreement Number 38637. The views expressed herein do not necessarily represent the views of the DOE or the U.S. Government.



*Cover Photos by Dennis Schroeder: (clockwise, left to right) NREL 51934, NREL 45897, NREL 42160, NREL 45891, NREL 48097, NREL 46526.*

# Performance Evaluation of Multi-Vendor Grid-Forming Inverters for Grid-Connected Operation Through Hardware Experimentation

Jing Wang, Subhankar Ganguly, Benjamin Kroposki
Power Systems Engineering Center, National Renewable Energy Laboratory
Golden, CO 80401, USA
{jing.wang, subhankar.ganguly, benjamin.kroposki}@nrel.gov

***Abstract*—Existing real-world projects of grid-forming (GFM) inverters that operate in parallel with power grids are typically sized between dozens and a few hundred megawatts, according to a recent white paper on GFM inverters by the North American Electric Reliability Corporation. These large systems are often difficult to evaluate prior to deployment because of their large size. The performance of smaller GFM inverters (from dozens to a few hundred kVA) that operate in parallel with power grids (distribution systems) is even less understood. There is an opportunity to better understand these systems through hardware testing under controlled laboratory conditions. Therefore, this paper presents the functional performance evaluation tests of multiple (three) commercial GFM inverters when they operate in parallel with the grid through hardware experiments. The goal of these tests is to explore and benchmark the GFM inverters' functionalities and dynamic response when they are operated in parallel with power grids to eventually develop universal specifications for GFM inverters. Both steady-state (changing the inverters' frequency and voltage droop) and transient (adding step changes to the grid's frequency/voltage) tests are performed for each GFM inverter with the same testing circuit and testing protocol. The experimental results indicate that 1) the GFM inverters can be dispatched through frequency and voltage droop intercepts to output the target power when they are operated in parallel with the grid; and 2) the GFM inverters automatically respond to system frequency and voltage events to output the needed power; however, all the GFM inverters show stability issues when absorbing reactive power from the grid.**

***Index Terms*—Grid-forming inverters, microgrids, parallel to the grid, performance evaluation.**

## I. INTRODUCTION

Research has shown that power grids dominated by inverter-based resources (IBRs) need grid-forming (GFM) IBRs to maintain stable operation due to the absence of supplemental synchronous machine-based solutions [1]. It is well-known that GFM IBRs are usually used for microgrid applications to black-start the system or transition to islanded operation to operate as the grid-forming source and maintain system voltage and frequency [2],[3],[4],[5]. Some island systems (e.g., Hawaiian Electric) already face IBR integration challenges and are starting to require the use of GFM inverters to improve system stability and strength [6]. Also, bulk transmission systems show a strong need to deploy GFM technology (e.g., synchronous condensers, GFM battery inverters) to maintain stable operation, especially in weak grid conditions. Overall, the need for GFM technology is increasing, which will accelerate with the rapid integration of renewable generation across North America and the world [7].

Existing real-world projects of GFM inverters that operate in parallel with power grids range in size from dozens to a few hundred megawatts, according to a recent white paper on GFM inverters by the North American Electric Reliability Corporation [7]. And the performance of smaller GFM inverters (from dozens to a few hundred kVA) that operate in parallel with power grid (distribution systems) has not been evaluated/understood to date, especially through the hardware setup. In future distribution systems, GFM inverters will be very important assets because of their capabilities to improve system stability and strength in power grids with high integration levels of renewable generation in addition to their capabilities for system restoration and black-start, which are mostly used today. In this paper, the laboratory hardware is set up to test a GFM inverter's stability in grid-connected mode with weak grid conditions [8]. The power control strategies of the GFM inverters operate in both GFM control grid-connected and islanded modes and are designed in [9] to achieve good control performance (power tracking, P-Q capability, and smooth transition operation) in grid-connected mode. A unified control algorithm for grid-tied and GFM battery inverters was developed to facilitate seamless transition operation without changing the inverter control algorithm [10].

To date, there has been little research related to smaller GFM inverters operating in grid-tied mode, and it has mostly been based on electromagnetic transient simulation; however, industry is requiring more hardware-related work (e.g., pure hardware evaluations and real-world pilot project demonstrations) to understand not only the GFM inverters' performance and advantages but also the expected performance and validation of the technology. As part of the Universal Interoperability for Grid-forming Inverters (UNIFI) Consortium, a hardware test bed has been set up to validate the performance of GFM IBRs. A goal of UNIFI Consortium is to validate and verify performance specifications that will enable GFM IBRs to be safely integrated into power grids with any amount of IBR

This work was authored by the National Renewable Energy Laboratory, operated by Alliance for Sustainable Energy, LLC, for the U.S. Department of Energy (DOE) under Contract No. DE-AC36-08GO28308. This material is based upon work supported by the U.S Department of Energy Office of Energy Efficiency and Renewable Energy Solar Energy Technologies Office Agreement Number 38637. The views expressed in the article do not necessarily represent the views of the DOE or the U.S. Government. 

TABLE I
Specifications of the three GFM inverters

| **Specification** | **GFM 1** | **GFM 2** | **GFM 3** |
|---|---|---|---|
| Frequency droop settings | 0.25% | 0.1 Hz gives 7.8 kW at 500 | 0.5 Hz |
| Frequency droop | 0.25% | 0.67% at 500 | 0.83% |
| Voltage droop settings | 5% | 10 V gives 7.22 kVar at 2,160 | 24 V |
| Voltage droop | 5% | 6.48% | 5% |
| Synch check | Yes (GCB and MCB) | No | Yes (GCB) |
| Secondary control | Yes | Yes | Yes |
| Operation mode | GFM, GFL, and grid-supporting control | GFL and GFM control | GFL and GFM control |
| Communication protocol | Modbus TCP | Modbus TCP | Modbus TCP |

and synchronous generators. Thus, this paper presents the functional performance evaluation tests of multiple (three) smaller, commercial GFM inverters when they are operated in parallel with the grid. Both steady-state (changing the inverters' frequency and voltage droop) and transient (adding step changes to the grid's frequency/voltage) testing are performed using the same testing circuit and testing protocol for each GFM inverter. The goal of this testing is to explore and benchmark the GFM inverters' functionalities and dynamic response when they are operated in parallel with the grid, especially during conditions when the system might not be stable. The results will inform the UNIFI specifications for GFM IBRs [11].

## II. GFM Inverter Performance Evaluation

This work is performed as part of UNIFI's Consortium's 1-MW multi-vendor GFM inverter experiment, in which seven GFM inverters from multiple vendors will be evaluated. Each individual GFM inverter will be evaluated in multiple operation modes, including stand-alone islanded operation, heterogeneous islanded (in parallel with a synchronous generator), grid-connected, and transition operations. This paper discusses the hardware evaluation of three GFM inverters (GFM 1, GFM 2, and GFM 3) operating in GFM control during grid-connected mode. The three inverters range in size from 30 kW to 250 kW. The results of individual inverters for other operational modes will be included in future project reports. Table I shows the specifications of the three GFM inverters.

Table II lists all the testing cases for grid-connected mode, including the steady-state and transient tests. For the steady-state sourcing in the active power case, the grid simulator supplies a resistive load equal to the size of the GFM inverter, then the GFM inverter is synchronized to the grid simulator and the load. The inverter frequency droop intercept is adjusted to achieve the target active power output. Similar to the steady-state sourcing in the active power case, the voltage droop intercept is adjusted to achieve the target reactive power output for the steady-state sourcing in the reactive power case. For the sinking power case, no load is applied, the inverter voltage droop is set to have zero reactive power flow, and the frequency droop intercept is adjusted to force the inverter to sink the target active power. For the transient frequency step test, the grid simulator is set to nominal voltage, and its frequency is stepped up or down from a real-time digital simulator (RTDS) to force the GFM inverter to generate the target active power, and the inverter voltage and frequency droop are kept the same at nominal. A similar configuration is used for the transient test voltage step of the grid simulator to force the inverter to generate the target reactive power.

TABLE II
Summary of all testing cases for grid-connected operation

| Test Type | Scenario | Test Approach |
|---|---|---|
| Steady state | Sourcing power | With the grid simulator set to nominal voltage and the frequency and inverter voltage droop curve intercepts set to achieve 0 or minimal reactive power flow, the inverter frequency droop curve intercept is adjusted to force the inverter to source 5%, 10%, 25%, 50%, 75%, and 100% rated kW. With the inverter frequency droop curve intercept set to achieve 0 or minimal real power flow, the voltage droop curve intercept is adjusted to force the inverter to source and sink 5%, 10%, 25%, 50%, 75%, and 100% rated kVAR. |
| | Sinking power | With the grid simulator set to nominal voltage and frequency and the inverter voltage droop curve intercepts set to achieve 0 or minimal reactive power flow, the inverter frequency droop curve intercept is adjusted to force the inverter to sink 25%, 50%, 75%, and 100% rated kW. |
| Transient | Frequency step | With the inverter voltage and frequency droop curve intercepts set to nominal values and the grid simulator voltage set to nominal value, the grid simulator frequency is stepped to force the inverter to source and sink 50% and 100% rated kW. |
| | Voltage step | With the inverter voltage and frequency droop curve intercepts set to nominal values and the grid simulator frequency set to nominal value, the grid simulator voltage is stepped to source and sink rated kVAR. |

To benchmark the performance of the GFM inverters, the same testing circuit is used to test the three GFM inverters. Fig. 1 shows the test setup, which includes the GFM inverter with a battery emulator on the DC side, a $\Delta : Y$ transformer, a point of point coupling (PCC) circuit breaker, a grid simulator (540-kVA) representing a strong grid connection, and a 250-kVA load bank. The RTDS is used to control the voltage reference in the grid simulator. A laptop is used as a controller to control and dispatch the GFM inverter, the load bank, and the PCC switch.

## III. Grid-Connected Mode Configuration

### *A. Steady-State Test*

In grid-connected mode, the grid voltage is dominant so that the GFM inverter has to follow the grid voltage. Assuming that the grid voltage is at 60 Hz, the inverter's operating point lands at zero active power and 60 Hz based on the droop curve, as shown in Fig.2a. When the inverter frequency droop intercept is shifted up, the active power flows from the GFM inverter to the grid. When the inverter frequency droop intercept is shifted down, the active power automatically flows from the grid to the

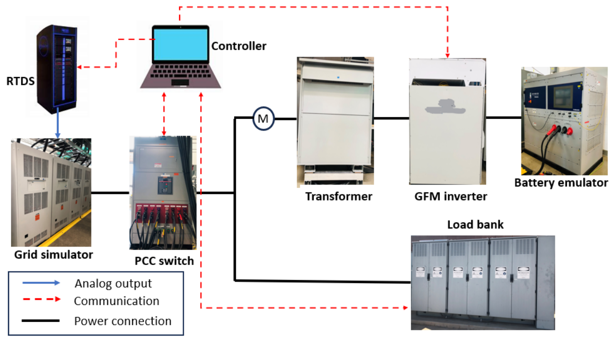


Fig. 1. Laboratory experiment setup. Photos by NREL

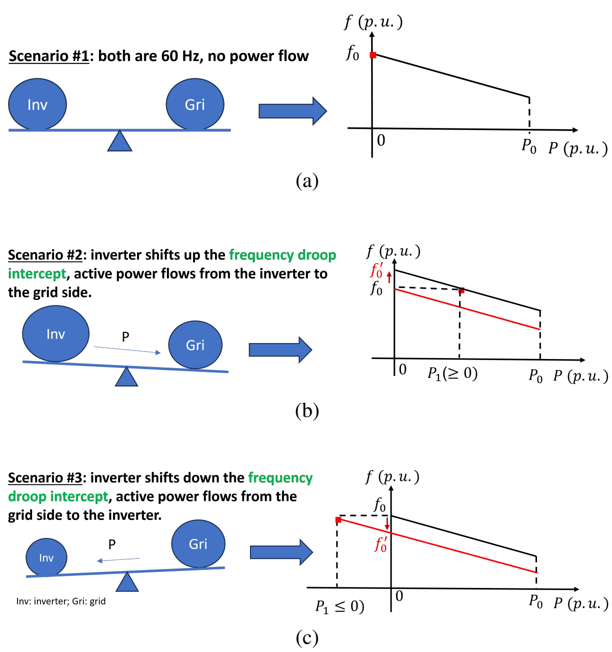


Fig. 2. Grid-connected operation: a) equal frequency, b) inverter frequency higher than the grid, and c) inverter frequency lower than the grid.

GFM inverter. This autonomous response of the GFM inverter enables the GFM inverter to respond to system frequency events much faster than grid-following (GFL) inverters. Fig.2 illustrates the principles of the dispatch of the GFM inverter frequency droop intercept to allow the inverter to output the target active power when it is operated in parallel with the grid. Overall, the relationship between the target output active power and the adjustment of the frequency droop is described as:

$$f^* = 60 + \Delta f = 60 + m * P * 60 \tag{1}$$

where $m$ is the frequency droop slope, and $P$ is the target active power in per unit (p.u.). In general, the active power of the inverter can be dispatched through adjusting the droop intercept.

Theoretically, the same principle can be used to allow the GFM inverter to output the target reactive power by adjusting the voltage droop intercept. The test from the stand-alone islanded mode showed that the voltage droop curves

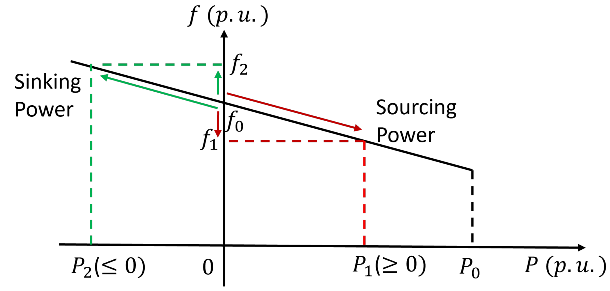


Fig. 3. Transient test—grid simulator frequency step up or down.

for the three GFM inverters are off nominal value, and the droop slopes change as well, as shown from (2)–(4). Because the measurement is at the transformer Y-side for the droop characterization test, the voltage at the transformer Y-side is different from the inverter terminal voltage; thus, the voltage droop is off.

$$GFM1 = \begin{cases} v^* = 0.9932 - 6\% * Q & (Q \geq 0) \\ v^* = 0.9955 - 4.4\% * Q & (Q \leq 0) \end{cases} \tag{2}$$

$$GFM2 = \begin{cases} v^* = 0.9972 - 6.8\% * Q & (Q \geq 0) \\ v^* = 0.9969 - 5.8\% * Q & (Q \leq 0) \end{cases} \tag{3}$$

$$GFM3 = \begin{cases} v^* = 1.0119 - 8.4\% * Q & (Q \geq 0) \\ v^* = 1.008 - 6.8\% * Q & (Q \leq 0) \end{cases} \tag{4}$$

Based on the correct voltage droop characteristic, the same principle can be applied for the voltage droop adjustment to allow the inverter to output the target reactive power, as expressed in (5). Note that the "nonunity" droop intercept needs to be included as well, otherwise the GFM inverter will not generate the target reactive power.

$$V^* = 480 + \Delta V = 480 + n * Q * 480 + (v_0 - 1) * 480 \tag{5}$$

where $v_0$ is the actual voltage droop intercept, $n$ is the actual droop slope, and $Q$ is the reactive power in per unit.

### *B. Transient Test*

In this test, the GFM inverter droop settings are maintained the same as in the characterization test, and the grid simulator frequency/voltage is varied to create the emulated frequency/voltage event to force the GFM inverter to output the desired amount of power. The RTDS is used to drive the step change of the voltage (frequency and voltage magnitude) of the grid simulator. Fig. 3 shows the example of varying the grid simulator frequency to force the GFM inverter to absorb or inject the target active power. Overall, if the goal is to force the inverter to generate the target power, $P$, the grid simulator frequency will be $f = 60 - m * P * 60$ Hz, where $m$ is the frequency droop slope, and $P$ is the target active power output; otherwise the grid simulator frequency will be $f = 60 + m * P * 60$ Hz to force the GFM inverter to absorb the target active power, $P$. Note that the voltage droop intercept needs to be dispatched to ensure that the reactive power flow of the GFM inverter is small.

To force the GFM inverter's output to the target reactive power, the grid simulator's voltage is stepped using an approach similar to that used during the steady-state testing. This is done by changing the inverter's droop intercept to output the target reactive power. For example, if the goal is to force the GFM inverter to inject the target reactive power, $Q$, the grid simulator needs to step down the voltage magnitude by $\Delta V = n_1 * Q * 277 - (1 - v_{01}) * 277$ ($Q \geq 0$), with $n_1$ as the droop slop and $v_01$ as the droop intercept, to inject the reactive power. If the goal is to force the GFM inverter to absorb the target reactive power, the grid simulator needs to step up its voltage magnitude by $\Delta V = n_2 * Q * 277 - (1 - v_{02}) * 277$ ($Q \leq 0$), with $n_2$ as the droop slop and $v_{02}$ as the droop intercept, to absorb the reactive power.

## IV. Experiment Results

For the three GFM inverters, the same testing circuit and testing protocols were used. Overall, the testing results matched the expectations.

### A. Steady-State Testing Results

The testing results for the three GFM inverters sourcing active power by shifting the frequency droop intercept up are summarized in Table III. The table summarizes the measured active power, the reactive power, and the current total harmonic distortion (THD) for each GFM inverter. The main observations are summarized as follows: 1) All three inverters can output the target active power, and the tracking error is acceptable. 2) Due to the voltage drop with higher active power, the inverters absorb a large amount of reactive power, which derates the inverter, and therefore the inverters might not be able to deliver 100% active power. 3) The THD of the inverter current is very high at lower power levels. 4) Only GFM 3's voltage droop intercept needed to be shifted down by 3 V to have near zero reactive power output. 5) There are no oscillations from any of the three GFM inverters. 6) GFM 2 has a large overshoot when the droop intercept is shifted up.

Table IV summarizes the testing results for the three GFM inverters sourcing reactive power by shifting the voltage droop intercept up. The main observations are summarized as follows: 1) All three inverters can output the target reactive power, and the tracking error is acceptable. 2) The active power output is small for all three inverters because the inverters maintain the frequency at 60 Hz. 3) The THD of the inverter current is very high at lower power levels and worse than the test with active power. 4) There are oscillations and overshoots in the current for GFM 1 when the droop intercept is shifted up, and the other two inverters show smooth transients.

Table V summarizes the testing results for the three GFM inverters sinking active power by shifting the frequency droop intercept down. The main observations are summarized as follows: 1) All three inverters can output the target reactive power, and the tracking error is acceptable. 2) The reactive power output is high at higher active power output; however, the inverters can still sink the target active power, and there is no derating of the inverters. 3) The THD of the inverter current is very high at lower power levels. 4) GFM 1 and GFM 3 have smooth transients when the droop intercept is shifted down, whereas GFM 2 has a large overshoot, especially for 25% (inverter has oscillations) and 100% (inverter tripped).

TABLE III
Inverter sourcing active power by shifting up the frequency droop intercept

| Target active power (p.u.) | | 0.05 | 0.1 | 0.25 | 0.5 | 0.75 | 1 |
|---|---|---|---|---|---|---|---|
| GFM 1 | P | 0.06 | 0.11 | 0.23 | 0.48 | 0.73 | 0.9 |
| | Q | -0.006 | -0.03 | -0.09 | -0.21 | -0.34 | -0.42 |
| | $THD_i$ (%) | 65.73 | 33.54 | 14.84 | 7.26 | 4.9 | 4.17 |
| GFM 2 | P | 0.02 | 0.08 | 0.23 | 0.48 | 0.73 | 0.98 |
| | Q | -0.06 | -0.07 | -0.1 | -0.15 | -0.21 | -0.27 |
| | $THD_i$ (%) | 51.06 | 39.34 | 10.12 | 5.33 | 4.01 | 3.92 |
| GFM 3 | P | 0.04 | 0.1 | 0.23 | 0.48 | 0.71 | 0.94 |
| | Q | -0.01 | -0.03 | -0.06 | -0.06 | -0.14 | -0.21 |
| | $THD_i$ (%) | 47.65 | 22.4 | 8.11 | 4.09 | 2.55 | 2.37 |

TABLE IV
Inverter sourcing reactive power by shifting up the voltage droop intercept

| Target reactive power (p.u.) | | 0.05 | 0.1 | 0.25 | 0.5 | 0.75 | 1 |
|---|---|---|---|---|---|---|---|
| GFM 1 | Q | 0.06 | 0.11 | 0.25 | 0.49 | 0.63 | 0.95 |
| | P | -0.02 | -0.02 | -0.01 | 0.007 | 0.02 | 0.05 |
| | $THD_i$ (%) | 51.42 | 33.26 | 14.29 | 7.96 | 6.52 | 5.57 |
| GFM 2 | Q | 0.01 | 0.04 | 0.2 | 0.45 | 0.69 | n/a |
| | P | -0.02 | -0.03 | -0.02 | -0.01 | -0.0006 | n/a |
| | $THD_i$ (%) | 51.06 | 39.34 | 10.12 | 5.33 | 4.01 | n/a |
| GFM 3 | Q | -0.002 | 0.06 | 0.21 | 0.48 | 0.73 | 0.95 |
| | P | -0.009 | -0.009 | 0.006 | 0.03 | 0.06 | 0.08 |
| | $THD_i$ (%) | 91.75 | 35.57 | 12.33 | 7.72 | 6.89 | 6.49 |

### B. Transient Testing Results

There are four sets of testing results for the transient testing: the grid simulator frequency stepping up and down and the grid simulator voltage magnitude stepping up and down. The results are shown in Table VI through Table VIII. when stepping down the grid simulator frequency, the three inverters could not complete the test to 100% because all the inverters tripped off. But the three inverters could generate the target active power for the other three operating points. Compared to the the respective results shown in Table III with the same operating point, GFM 1 has a better current THD, GFM 2 has worse current THD, and GFM 3 has a similar THD. The reason that the inverters tripped off was because of overcurrent. This is most likely because the provision of reactive power output derates the inverter; however, the difference in frequency forces the inverter to reach the new operating point.

When stepping up the grid simulator's frequency, GFM 1 is able to complete all the testings, whereas the other two can only complete the first three tests. Similar observations are made compared to the test shifting the inverter frequency droop down to sink power, as outlined in Table V. For GFM 1, this testing showed a better current THD, whereas the other

TABLE V
Inverter sinking active power by shifting down the frequency droop intercept

| Target active power (p.u.) | | -0.05 | -0.1 | -0.25 | -0.5 | -0.75 | -1 |
|---|---|---|---|---|---|---|---|
| GFM 1 | P | -0.07 | -0.12 | -0.26 | -0.51 | -0.77 | -1 |
| | Q | -0.02 | 0.002 | 0.05 | 0.14 | 0.23 | 0.32 |
| | $THD_i$ (%) | 47.37 | 27.13 | 13.35 | 6.61 | 4.42 | 3.44 |
| GFM 2 | P | n/a | -0.12 | -0.28 | -0.54 | -0.79 | n/a |
| | Q | n/a | -0.05 | -0.01 | 0.03 | 0.08 | n/a |
| | $THD_i$ (%) | n/a | 24.18 | 12.3 | 8.01 | 5.52 | n/a |
| GFM 3 | P | -0.07 | -0.12 | -0.26 | -0.5 | -0.75 | -0.96 |
| | Q | 0.006 | 0.02 | 0.06 | 0.14 | 0.21 | 0.28 |
| | $THD_i$ (%) | 27.32 | 17.36 | 6.87 | 4.51 | 3.26 | 2.81 |

TABLE VI
Inverter sourcing active power by stepping down the grid simulator frequency

| Target active power (p.u.) | | 0.25 | 0.5 | 0.75 | 1 |
|---|---|---|---|---|---|
| GFM 1 | P | 0.22 | 0.47 | 0.74 | n/a |
| | Q | -0.14 | -0.25 | -0.21 | n/a |
| | $THD_i$ (%) | 5.06 | 5.05 | 3.87 | n/a |
| GFM 2 | P | 0.24 | 0.5 | 0.74 | n/a |
| | Q | -0.09 | -0.11 | -0.16 | n/a |
| | $THD_i$ (%) | 11.29 | 10.27 | 13.21 | n/a |
| GFM 3 | P | 0.24 | 0.47 | 0.7 | n/a |
| | Q | -0.1 | -0.17 | -0.25 | n/a |
| | $THD_i$ (%) | 9.87 | 3.77 | 2.71 | n/a |

TABLE VII
Inverter sinking active power by stepping up the grid simulator frequency

| Target active power (p.u.) | | -0.25 | -0.5 | -0.75 | -1 |
|---|---|---|---|---|---|
| GFM 1 | P | -0.25 | -0.5 | -0.75 | -1 |
| | Q | -0.002 | 0.09 | 0.18 | 0.26 |
| | $THD_i$ (%) | 5.27 | 5.27 | 3.4 | 2.54 |
| GFM 2 | P | -0.28 | -0.53 | -0.79 | n/a |
| | Q | 0.02 | 0.07 | 0.12 | n/a |
| | $THD_i$ (%) | 14.57 | 11.74 | 14.7 | n/a |
| GFM 3 | P | -0.24 | -0.49 | -0.74 | n/a |
| | Q | 0.05 | 0.13 | 0.2 | n/a |
| | $THD_i$ (%) | 11.87 | 5.0 | 3.64 | n/a |

two GFM inverters have a worse current THD than the prior testing. The results shown here indicate that the change in the grid frequency automatically forces the GFM inverters to output the corresponding active power for real-world electric grids. The settling times for the three GFM inverters are less than 0.5 s for GFM 1, less than 6 s for GFM 2, and less than 1 s for GFM 3.

When stepping down the grid simulator's voltage magnitude, the inverter has a noticeable tracking error compared to the case shifting up the voltage droop intercept. This is because the inverter's voltage is lower after injecting the reactive power, and the reactive power is therefore lower than expected. For all three inverters, the current THD exceeds 5%. Also, oscillations are observed only for the first GFM inverter when the grid simulator is stepping down the voltage. The settling times for the three GFM inverters are less than 0.4 s for GFM 1, less than 2 s for GFM 2, and less than 0.7 s for GFM 3.

When stepping up the grid simulator's voltage magnitude, all three inverters show oscillations after the grid simulator steps up the voltage for all the operating points, and the system cannot reach steady state. The larger the change in voltage, the worse the oscillations. This indicates that the inverters have high volt/var sensitivity at high power importing levels.

## V. Conclusions

This paper presents the individual laboratory experimental results from testing three commercial, off-the-shelf GFM inverters' performance while operating in parallel with the grid (emulated by a grid simulator). The goal is to benchmark the inverters' response when operating GFM inverters in parallel with electric grids through some representative testing. Both steady-state (changing the droop intercept of each GFM inverter) and transient (step up/down of the grid simulator's frequency/voltage) testing were performed. The steady-state testing showed that the GFM inverters can be dispatched through the voltage and frequency droop intercepts to output the target power, similar to how GFL inverters are directly dispatched through active and reactive power references. The transient testing showed the frequency and voltage responses of each GFM inverter when there is a dynamic change in the grid's frequency and voltage, and the GFM inverters automatically follow the grid's frequency/voltage to contribute active/reactive power. This testing also showed that the GFM inverters have stability issues when absorbing reactive power from the grid. The laboratory hardware testing is very helpful to explore and benchmark the GFM inverters' functionalities and dynamic response when operating in parallel with power grids. Future testing will evaluate multiple GFM inverters in parallel with the grid simulator and more dynamic testing, including phase jumps. As specifications for GFM inverters are being developed around the world, this testing can provide information on the feasibility of actual hardware testing and can also provide information on GFM control settings that can influence performance. Further, this testing is useful to provide feedback to manufacturers to improve GFM inverters and to ensure that the inverters can be seamlessly integrated into power grid operations.

TABLE VIII
Inverter sourcing reactive power by stepping down the grid simulator voltage

| Target reactive power (p.u.) | | 0.25 | 0.5 | 0.75 | 1 |
|---|---|---|---|---|---|
| GFM 1 | Q | 0.21 | 0.42 | 0.64 | 0.87 |
| | P | 0.0008 | 0.014 | 0.033 | 0.059 |
| | $THD_i$ (%) | 11.93 | 6.06 | 4.07 | 3.15 |
| GFM 2 | Q | 0.19 | 0.42 | 0.6 | n/a |
| | P | -0.009 | -0.007 | 0.007 | n/a |
| | $THD_i$ (%) | 18.97 | 9.71 | 6.25 | n/a |
| GFM 3 | Q | 0.24 | 0.47 | 0.68 | 0.9 |
| | P | 0.02 | 0.04 | 0.06 | 0.08 |
| | $THD_i$ (%) | 14.04 | 7.93 | 6.76 | 6.11 |

## References


[1] J. Matevosyan *et al.*, "Grid-forming technology in energy systems integration," Tech. Rep., Mar. 2022.

[2] Y. Lin *et al.*, "Research roadmap on grid-forming inverters," Tech. Rep. NREL/TP-5D00-73476, Dec. 2020.

[3] J. Wang, N. C. P. Chang, X. Feng, and A. Monti, "Design of a generalized control algorithm for parallel inverters for smooth microgrid transition operation," *IEEE Transactions on Industrial Electronics*, vol. 62, no. 8, pp. 4900–4914, 2015.

[4] J. Wang, A. Pratt, and M. Baggu, "Design of an advanced energy management system for microgrid control using a state machine," *Applied Energy*, vol. 228, pp. 2407–2421, 2018.

[5] Y. N. Velaga, J. Wang, A. Pratt, L. Abcede, and N. Shamukh, "Transient stability study of a real-world microgrid with 100*2022 IEEE Energy Conversion Congress and Exposition (ECCE)*. IEEE, 2022, pp. 1–8.

[6] Li Yu and Ken Aramaki. Hawaiian electric's plans for meeting clean energy targets and role of grid forming inverters. ESIG Webinar.

[7] A. Hoke *et al.*, "Grid forming functional specifications for bps-connected battery energy storage systems," Tech. Rep., 2023.

[8] R. Mittal, Z. Miao, and L. Fan, "Grid forming inverter: Laboratory-scale hardware test bed setup and weak grid operation," in *2021 North American Power Symposium (NAPS)*. IEEE, 2021, pp. 1–5.

[9] J. Wang, "Design power control strategies of grid-forming inverters for microgrid application," in *2021 IEEE Energy Conversion Congress and Exposition (ECCE)*. IEEE, 2021, pp. 1–8.

[10] M. R. Khan, M. A. Rahmani, M. E. Sied, and C. E. C. Gonzalez, "Design of a unified controller framework for grid-tied and grid-forming battery energy storage system," in *2022 – 48th Annual Conference of the IEEE Industrial Electronics Society (IECON)*. IEEE, 2022, pp. 1–6.

[11] K. Benjamin *et al.*, "Unifi specifications for grid-forming inverter-based resources—version 1," Tech. Rep. NREL/TP-5D00-73476, Dec. 2022.